1

Effects of scattering on fast electron transport in solid targets diagnosed via proton emission

Contact p.mckenna@phys.strath.ac.uk

M. N. Quinn, X. H. Yuan*, D. C. Carroll, P. Gallegos# and P. McKenna
SUPA Department of Physics, University of Strathclyde, Glasgow G4 0NG, UK
* also at State Key Laboratory of Transient Optics and Photonics, Xi'an Institute of Optics and Precision Mechanics, CAS, Xi'an 710119, China
# also at Central Laser Facility, STFC, Rutherford Appleton Laboratory

A. P. L. Robinson, R. J. Clarke and D. Neely
Central Laser Facility, STFC, Rutherford Appleton Laboratory, HSIC, Didcot, Oxon OX11 0QX, UK

R. G. Evans
The Blackett Laboratory, Imperial College London, London SW7 2 BZ, UK
(also at Central Laser Facility, STFC, Rutherford Appleton Laboratory)

L. Romagnani, K. Quinn, P. A. Wilson, G. Sarri and M. Borghesi
Department of Physics and Astronomy, Queen's University Belfast, Belfast BT7 1NN, UK

L. Lancia and J. Fuchs
LULI, École Polytechnique-Université Paris VI, 91128 Palaiseau, France

Introduction

In the interaction of a high power laser pulse with a solid density target a significant fraction of the laser energy is converted to relativistic electrons. The efficient transport of these fast electrons through the dense plasma is important for the Fast Ignition (FI) approach to Inertial Confinement Fusion [1], and for the development of laser-driven ion sources based on sheath acceleration at the target rear surface. The fast electron current far exceeds the Alfvén limit, and can only propagate because it is charge neutralized by a cold return current. The overlapped counter-propagating currents become unstable, both to longitudinal (two stream) and transverse (Weibel) instability modes, as reported upon a number of theoretical studies [2,3]. These instabilities lead to the filamentation of the fast electron beam.

Target	Z_{eff}	η_R [Ω.m]	$\alpha\gamma_f/\nu$
Au	79	10^{-8}	0.02
SiO_2	15	10^{14}	1.5
Al	13	10^{-7}	3.7
CH	3	10^{13}	81
Li	3	10^{-7}	360

Table 1. Target material properties: Effective atomic number Z_{eff}, room temperature resistivity η_R and transverse instability growth factor r$\alpha\gamma_f/\nu$ (described in main text).

The large differences between electron transport instabilities in low Z targets (such as CH) and moderate Z targets (such as Al) are not well understood. For plastic targets (CH), the effect is traditionally attributed to the target being initially an insulator. However, at solid densities angular scattering of the beam electrons in the background plasma can be significant. Higher Z materials, such as aluminium, induce sufficient angular scattering, raising the transverse temperature of the electron beam, which could reduce the tendency for it to filament [4,5]. The overall filament growth before being stabilised is determined by the quantity $\alpha\gamma_f/\nu$, where α is the ratio of fast electron beam density to background density, γ_f is the normalised growth rate for the filamentation (approximately the beam plasma frequency) and ν is the normalised growth rate of transverse temperature. Sample values of $\alpha\gamma_f/\nu$ for test materials are shown in Table 1. High values imply large filament growth. However, this model only evaluates the scattering effects within the electron beam, the influence of material resistivity and the collisional return current are not included.

We report here on the results of an experiment aimed at resolving the relative importance of atomic number and resistivity on the differences in electron transport in CH and Al targets. This is achieved by comparing electron transport patterns in the range of targets listed in Table 1, including the low-Z metallic foil Li and moderate-Z insulator SiO_2.

Experiment

The experiment was performed using the Vulcan petawatt laser. The laser delivered p-polarised pulses of wavelength equal to 1.053 µm, with energy up to 280 J (on target) and pulse duration equal to 700 fs (FWHM). The pulses were focused to a calculated peak intensity of 6×10^{20} W/cm^2. The targets, as listed in Table 1, were prepared to micron-scale surface smoothness by employing a lapping technique. The target thickness was varied in the range 25 µm to 1.4 mm. Three types of lithium (Li) target were used: (1) uncoated Li; (2) Li with a 2 µm CH coating on both surfaces; (3) Li with a flash (50 nm) coating of Au on both surfaces.

Diagnosing the transport of fast electrons in solid targets is inherently difficult. The experimental challenge to observe signatures of electron-bunching at the rear surface of the target, resulting from

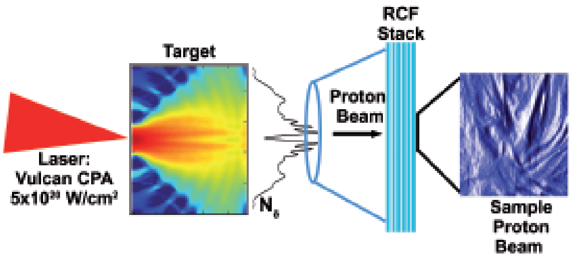

Figure 1. Experimental arrangement demonstrating fast electron transport within the target (generated by a 2-D simulation using the LEDA code) and the proton emission detection method.

filamentation, was met using high resolution measurements of proton emission by the TNSA (Target Normal Sheath Acceleration) mechanism [6]. Measurement of multi-MeV proton emission has been shown to be a sensitive diagnostic of fast electrons [7]. TNSA is the dominant ion acceleration mechanism for the laser and target parameters of this experiment, as shown using targets with a groove structure machined in the rear surface, which is reproduced in the expanding ion front, and by efficient carbon and oxygen ion acceleration from layers on the target rear surface. The primary detector used was passive stacks of dosimetry (RCF) film, which enable the spatial intensity distribution of the proton beam to be measured at given energies. The experimental arrangement is shown in Fig. 1.

Results and discussion

The results of the experiment will be presented in detail elsewhere [8]. Briefly, the RCF was analysed to quantify the degree of variance in the proton signal and hence the degree of filamentation of the electron distribution forming the sheath at the target rear surface. Multiple regions of the proton spatial intensity profile were sampled around the centre of the beam where the proton beam laminarity is maximum [9]. The 2D variance of the proton signal was measured at 50% of the maximum beam energy for each target material. We estimate the transverse size of the electron filamentary structures at the target rear surface by comparing the results with measured proton dose distributions from targets with a periodic structure engineered into the rear surface [10].

Figure 2 shows results from the proton beam variance analysis. The data set for this analysis comprised of the targets listed in Table 1. The experimental measurements show that the insulator targets produce the greatest degree of filamentation which is in agreement with previous results [7]. It is also observed that the degree of filamentation increases with target thickness up to 600 µm for CH. Importantly, by comparing the Li and Al results, we see that for a similar initial resistivity, the variation in effective Z makes no measurable difference to the beam structure, suggesting that scattering plays little role in suppressing filamentation. An estimate of the transverse size of the beam inhomogeneities gives an upper limit of ~1 µm for the metal targets and 4–5 µm for the insulator targets.

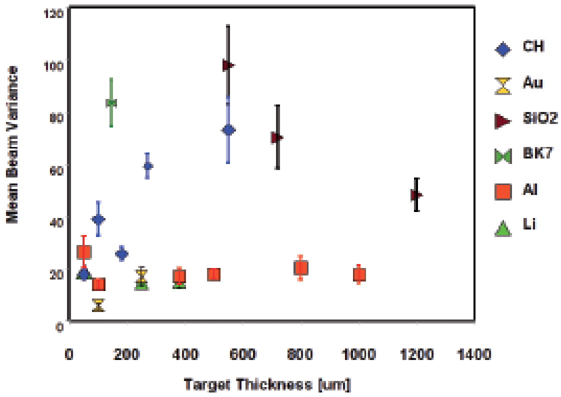

Figure 2. Proton beam variance as a function of target thickness for the various target materials used. The error-bars represent the fluctuations in variance over a number of sample points across the proton beam.

Summary

An experiment was carried out using the Vulcan Petawatt laser to resolve the debate regarding the effect of scattering in suppressing filamentation growth in fast electron transport in solid targets. The results suggest that scattering plays little role in suppressing electron beam propagation instabilities. A programme of simulation runs to model the conditions of the experiment is in progress and will be reported in a future publication.

Acknowledgements

The authors would like to acknowledge the scientific and technical support of the staff at the Central Laser Facility. The authors also thank Dr. R. Martin for his help in using a computer cluster at the University of Strathclyde. This work is funded by ESPRC Grant No. EP/E048668/1 and the EU COST P-14 Action.

References

1. M. Tabak *et al.*, *Phys. Plasmas* **1**, 1626 (1994).
2. A. Bret, M. C. Firpo, and C. Deutsch, *Phys. Rev. Lett*. **94**, 115002 (2005).
3. M. Honda, *Phys. Rev. E* **69**, 016401 (2004).
4. R. G. Evans, *Plasma Phys. Controll. Fusion* **49**, B87 (2007).
5. L. O. Silva *et al.*, *Phys. Plasmas* **9**, 2458 (2002).
6. S. C. Wilks *et al.*, *Phys. Plasmas* **8**, 542 (2001).
7. J. Fuchs *et al.*, *Phys. Rev. Lett*. **91**, 255002 (2003).
8. M. N. Quinn *et al.*, in preparation.
9. T. E. Cowan *et al.*, *Phys. Rev. Lett*. **92**, 204801 (2004).
10. F. Nurnberg *et al.*, *Rev. Sci. Instrum*. **80**, 033301 (2009).